Sulfonated Polyaniline Nanostructures Synthesized via Rapid Initiated Copolymerization with Controllable Morphology, Size, and Electrical Properties

ARTICLE *in* MACROMOLECULES · FEBRUARY 2012

Impact Factor: 5.8 · DOI: 10.1021/ma2024446

Macromolecules

Article

pubs.acs.org/Macromolecules

Sulfonated Polyaniline Nanostructures Synthesized via Rapid Initiated Copolymerization with Controllable Morphology, Size, and Electrical Properties

Yaozu Liao,[†,‡,§] Veronica Strong,[§] Wei Chian,[†] Xia Wang,*[,†] Xin-Gui Li,[‡] and Richard B. Kaner*[,§]

[†]School of Materials Science and Engineering, University of Shanghai for Science and Technology, 516 Jun-Gong Road, Shanghai 200093, China

[‡]Institute of Materials Chemistry, College of Materials Science and Engineering, Tongji University, 1239 Si-Ping Road, Shanghai 200092, China

[§]Department of Chemistry and Biochemistry and California NanoSystems Institute, University of California, Los Angeles, Los Angeles, California, 90095-1569

ABSTRACT: Sulfonated polyaniline (SPANi), a self-doped conjugated polymer, has received great interest in recent years; however, controlling its shape, size, and conductivity at the nanoscale remains a significant challenge. Here, we report an initiator-assisted route to SPANi nanostructures by rapidly copolymerizing *o*-aminobenzenesulfonic acid with aniline or its derivatives in the presence of a catalytic amount of the initiator−aniline dimer. UV−vis, FT-IR, and XRD spectra reveal that the chemical compositions of the SPANi nanostructures are similar to that of conventional SPANi possessing an agglomerated morphology. By regulating the comonomer molar ratios, the aniline derivatives used and the acidic media employed, the morphology of the SPANi changes from 1-D nanofibers, nanosticks, nanothorns, and nanorods to 2-D nanoplates and 3-D porous nanospheres. The length and aspect ratio of the SPANi nanofibers can reach values up to 4.5 μm and 60, respectively. These SPANi nanostructures are readily processable in both organic and aqueous solvents and demonstrate 6 orders of magnitude enhanced conductivity at pH values of 5.5−6.0 when compared to conventional polyaniline.

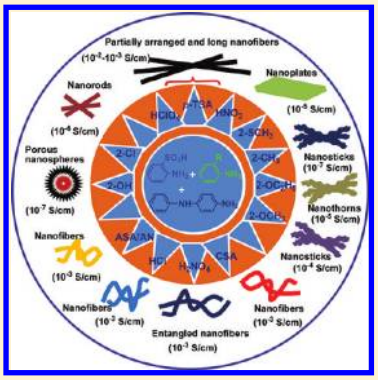

Polyaniline (PANi) is one of the most widely studied conducting polymers because of its facile synthesis, excellent chemical and environmental stability and good electrical conductivity leading to many potential applications such as lightweight battery electrodes, electromagnetic shielding, anticorrosion coatings, and sensors.[1,2] Limited processability and loss of electrochemical activity at neutral pH are arguably two of the biggest problems for its utilization in fields such as bioelectrochemistry and biomaterials. Fabrication of nanostructured PANi including nanoparticles, nanowires, nanofibers, nanotubes, and nanocomposites has been well developed by chemical methods to improve its water processability.[3,4] In particular, nanostructures of PANi offer the possibility of enhanced performance wherever a high interfacial area between PANi and its environment is needed. For example, in sensor applications, PANi nanofibers display much higher sensitivities and faster time responses relative to their conventional bulk counterparts due to higher effective surface areas and shorter penetration depths for target molecules.[5] Since most biomolecules such as enzymes are only stable and bioactive at neutral pH, it is critical to develop a form of PANi that does not deprotonate and become insulating under these conditions.[6] Despite improvements in water-processability and functionalities achieved by nanofabricating PANi, maintaining electrochemical activity in solutions of pH > 4.0 has only met with limited success so far.

Scheme 1. General Chemical Route to a Variety of Sulfonated Polyanilines (SPANi)

One derivative, known as self-doped PANi, has received much interest because the dopants are bound directly to the polymer backbone, in contrast to conventional polyaniline, which uses external dopants. Self-doped PANi typically exhibits conductivity of 10^{-6}−10^{-1} S/cm,[7−12] and several advantages, including improved solubility, electrical properties and redox activity over a wide pH range. For example, unsubstituted PANi becomes insulating at pH values greater than 4, while the conductivities of 50% and 75% sulfonated PANis are pH-independent up to pHs of 7.5 and ≤14,[12] respectively. Thus, self-doped PANi is considered a promising conjugated polymer for applications in the areas of rechargeable batteries,[13]

Received: November 4, 2011
Revised: January 15, 2012
Published: January 31, 2012

dx.doi.org/10.1021/ma2024446 | *Macromolecules* 2012, 45, 1570−1579

Table 1. Effect of ASA/Aniline Synthesized in 1.0 M HCl at Varying Molar Ratios on the Nanomorphology, Average Diameter (D_a), Average Length (L_a), Aspect Ratio (L_a/D_a), UV−Vis Absorbance Maximum (λ_{max}), Product Yield, and Conductivity of SPANi

ASA/aniline molar ratios	nanomorphology	D_a (nm)	L_a (μm)	L_a/D_a	λ_{max} (nm)	yield (%)	conductivity (S/cm)
0/100	nanofibers	50	1.0	20.0	790	45.9	3.3×10^{-8}
30/70	nanofibers	55	0.95	17.2	845	43.3	2.4×10^{-3}
50/50	nanofibers	55	0.75	13.6	856	34.5	3.0×10^{-3}
70/30	nanofibers	60	0.7	11.7	870	20.4	5.7×10^{-3}

Table 2. Effect of Acidic Media on the Nanomorphology, Average Diameter (D_a), Average Length (L_a), Aspect Ratio (L_a/D_a), UV−Vis Absorbance Maxima (λ_{max}), Product Yield, and Conductivity of SPANi When Using a 50/50 Ratio of ASA/Aniline

acidic media	nanomorphology	D_a (nm)	L_a (μm)	L_a/D_a	λ_{max} (nm)	yield (%)	conductivity (S/cm)
HCl	nanofibers	55	0.75	13.6	856	34.5	3.0×10^{-3}
HNO_3	nanofibers	55	1.8	32.7	858	28.5	1.2×10^{-2}
H_2SO_4	nanofibers	62	2.1	33.9	853	28.3	1.9×10^{-3}
CSA	nanofibers	65	1.2	18.5	853	32.4	1.9×10^{-3}
$HClO_4$	nanofibers	88	4.0	45.5	920	29.9	3.7×10^{-3}
p-TSA	nanofibers	75	4.5	60.0	873	27.1	4.5×10^{-3}

Table 3. Effect of 2-Substituents of Aniline Derivatives on the Nanomorphology, Average Diameter (D_a), Average Length (L_a), UV−Vis Absorbance Maxima (λ_{max}), Product Yield and Conductivity of SPANi Using 1.0 M HCl

2-substituents	nanomorphology	D_a (nm)	L_a (μm)	L_a/D_a	λ_{max} (nm)	yield (%)	conductivity (S/cm)
OH	nanospheres	400	–	–	418	7.8	2.9×10^{-7}
SCH_3	nanoplates	30 nm thick		–	858	22.8	1.4×10^{-5}
OCH_3	nanosticks	75	1.5	20.0	870	32.9	8.3×10^{-4}
Cl	nanorods	60	0.4	6.7	765	1.7	3.3×10^{-6}
OC_2H_5	nanothorns	63	0.8	12.7	873	30.8	6.9×10^{-5}
CH_3	nanofibers	52	0.7	13.5	825	24.2	6.0×10^{-7}

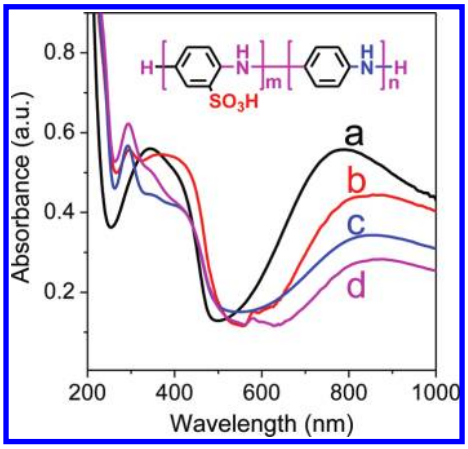

Figure 1. UV−vis spectra of SPANi synthesized with the following ASA/aniline molar ratios: (a) 0/100, (b) 30/100, (c) 50/50, and (d) 70/100 in the presence of 2.5 mol % *N*-phenyl-*p*-phenylenediamine per comonomer in 1.0 mol/L HCl.

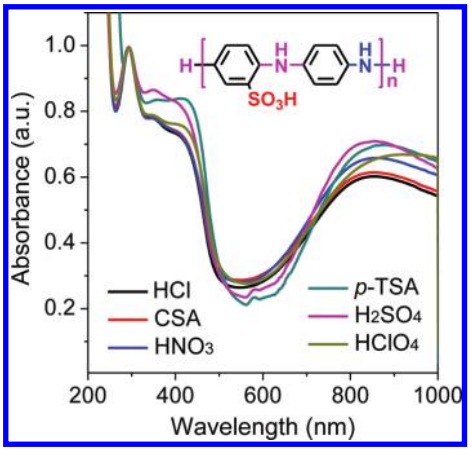

Figure 2. UV−vis spectra of SPANi synthesized in the following acidic medium: HCl (black line), HNO_3 (blue line), H_2SO_4 (magenta line), $HClO_4$ (dark yellow line), CSA (red line), or *p*-TSA (dark cyan line) in the presence of 2.5 mol % *N*-phenyl-*p*-phenylenediamine per comonomer in 1.0 mol/L HCl, at a fixed ASA/aniline molar ratio of 50/50.

light-emitting diodes,[14] biosensors,[15,16] cell scaffolds,[17] junction devices,[18] and electrochromics.[19] Examples of self-doped PANi syntheses include the introduction of sulfonic acid,[11,12,20,21] boronic acid,[22,23] carboxylic acid,[24] or phosphonic acid groups[25] into PANi either directly onto the aniline rings or on the side chains. These approaches have proved to be useful to enhance water-solubility and maintain electrochemical activity at neutral pH. Although significant progress has been made in the syntheses of self-doped PANi, there remains many limitations such as low yield, limited processability and poor mechanical, thermal and environmental stabilities. More importantly, no method has yet been developed that enables nanostructures of self-doped PANi to be varied systematically.

In this work, we report a rapid initiated copolymerization technique that produces self-doped sulfonated polyaniline (SPANi) with well-defined, controllable nanomorphologies, sizes, dimensionalities, and electric properties. Specifically, we report a new copolymerization approach using *o*-aminobenzenesulfonic acid (ASA) with aniline or aniline derivatives in the presence of a catalytic amount of the initiator *N*-phenyl-*p*-phenylenediamine (aniline dimer). The initiator accelerates the polymerization rate,

dx.doi.org/10.1021/ma2024446 | *Macromolecules* 2012, 45, 1570−1579

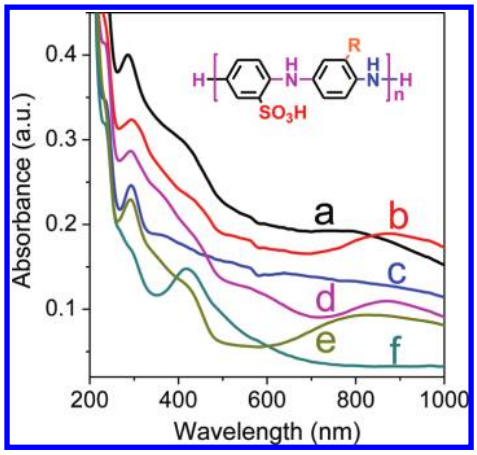

Figure 3. UV−vis spectra of SPANi synthesized with the following 2-substituted group (R) on aniline: (a) Cl, (b) OCH_3, (c) SCH_3, (d) OC_2H_5, (e) CH_3, or (f) OH in the presence of 2.5 mol % *N*-phenyl-*p*-phenylenediamine per comonomer in 1.0 mol/L HCl, at a fixed ASA/aniline molar ratio of 50/50.

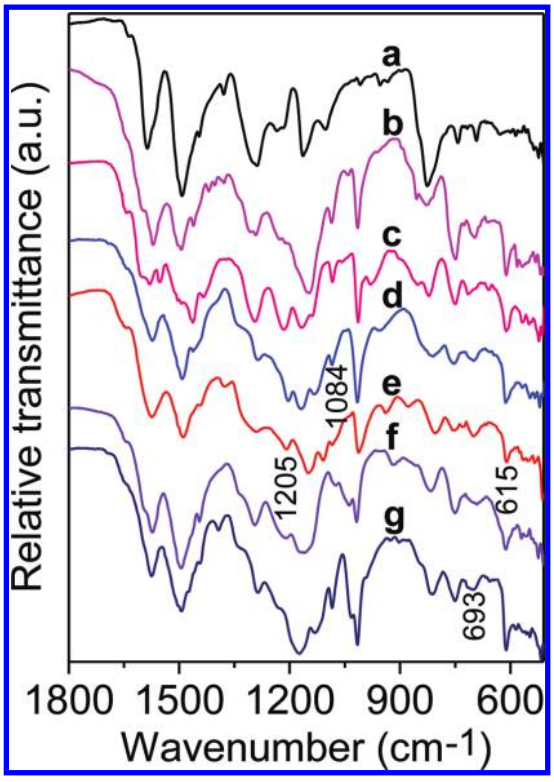

Figure 4. ATR/FT-IR spectra of (a) pristine PANi and (b−g) SPANi synthesized with the following 2-substituted group (R) on aniline: (b) Cl, (c) CH_3, (d) OH, (e), OCH_3, (f) SCH_3, or (g) OC_2H_5 in the presence of 2.5 mol % *N*-phenyl-*p*-phenylenediamine per comonomer in 1.0 mol/L HCl, at a fixed ASA/aniline ratio of 50/50.

which favors homogeneous nucleation and leads to the formation of PANi nanofibers.[2] The initiator molecules are believed to serve as nucleation centers for the growth of polymeric chains leading to the SPANi nanostructures. The effects of several important copolymerization parameters, including the comonomer ratios, aniline derivatives used and acidic media employed, on the product yields, chemical compositions, morphologies, sizes, dimensionalities, and electrical properties of the SPANi nanostructures are investigated in detail.

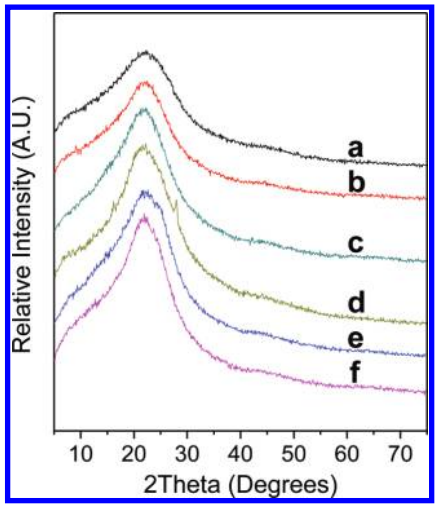

Figure 5. XRD patterns of SPANi synthesized in the following acidic media: (a) HCl, (b) HNO_3, (c) H_2SO_4, (d) $HClO_4$, (e) CSA, or (f) *p*-TSA in the presence of 2.5 mol % *N*-phenyl-*p*-phenylenediamine per comonomer in 1.0 mol/L HCl, at a fixed ASA/aniline molar ratio of 50/50.

EXPERIMENTAL SECTION

Synthesis of SPANi Nanostructures. All chemicals were of analytical grade and used as received. The SPANi nanostructures were synthesized by chemical oxidative copolymerization of ASA and aniline or aniline derivatives in the presence of 2.5 mol % (relative to the comonomers) of the aniline dimer and acidic medium. A general chemical route to a variety of SPANi derivatives is shown in Scheme 1. Typically, 2.5 mmol of ASA and 2.5 mmol of aniline were dissolved in 25 mL of 1.0 M HCl. The initiator (0.125 mmol) was predissolved in 1.0 mL of ethanol and mixed with the comonomer solution. An oxidant solution consisting of 5.0 mmol of ammonium peroxydisulfate (APS) and 25 mL of 1.0 M HCl were rapidly added to the comonomer solution. The reaction mixture was vigorously shaken for ∼10 s and then left undisturbed for 24 h. The crude product of SPANi nanofibers was purified by dialysis against deionized (DI) water at a constant pH of 5.5−6.0 for approximately two months. Finally, the SPANi powder was obtained by further drying the crude product at 50 °C in a vacuum oven for 72 h. By regulating the ASA/aniline molar ratios, aniline derivatives used and acidic media employed, the rapid initiated copolymerization method produced 1-D nanofibers, nanosticks, nanothorns, and nanorods, 2-D nanoplates, and 3-D porous nanospheres of SPANi. If not specifically mentioned, all experiments were performed using 1.0 M HCl as the acidic medium.

Chemical Composition, Morphology, and Conductivity. The SPANi nanostructures dispersed in DI water and/or dried SPANi powders were utilized for characterization of chemical composition, morphology and conductivity. Ultraviolet−visible (UV−vis) absorption spectra of SPANi nanostructures dispersed in DI water were recorded on an HP 8453 spectrometer. Attenuated Total Reflection Fourier transform infrared (ATR-FT-IR) spectra of dried SPANi powders were taken with a JASCO FT-IR 420 spectrometer. X-ray diffraction (XRD) spectra of the samples were scanned on a Philips X'pert Pro powder diffractometer by using copper-monochromatized CuKα radiation (λ = 1.54178 Å). Samples for a JEOL JSM-6700 field emission scanning electron microscope (SEM) were prepared on silicon wafers. Samples for a PHILIPS CM120 transmission electron microscope (TEM) were prepared on Formvar-coated copper grids. To investigate the electrical properties, the SPANi nanostructures were cast as thin films and measured using a two-point probe technique.[26]

RESULTS AND DISCUSSION

Product Yield, Conductivity, and Dispersibility. The effect of ASA/aniline molar ratios on the morphology, size,

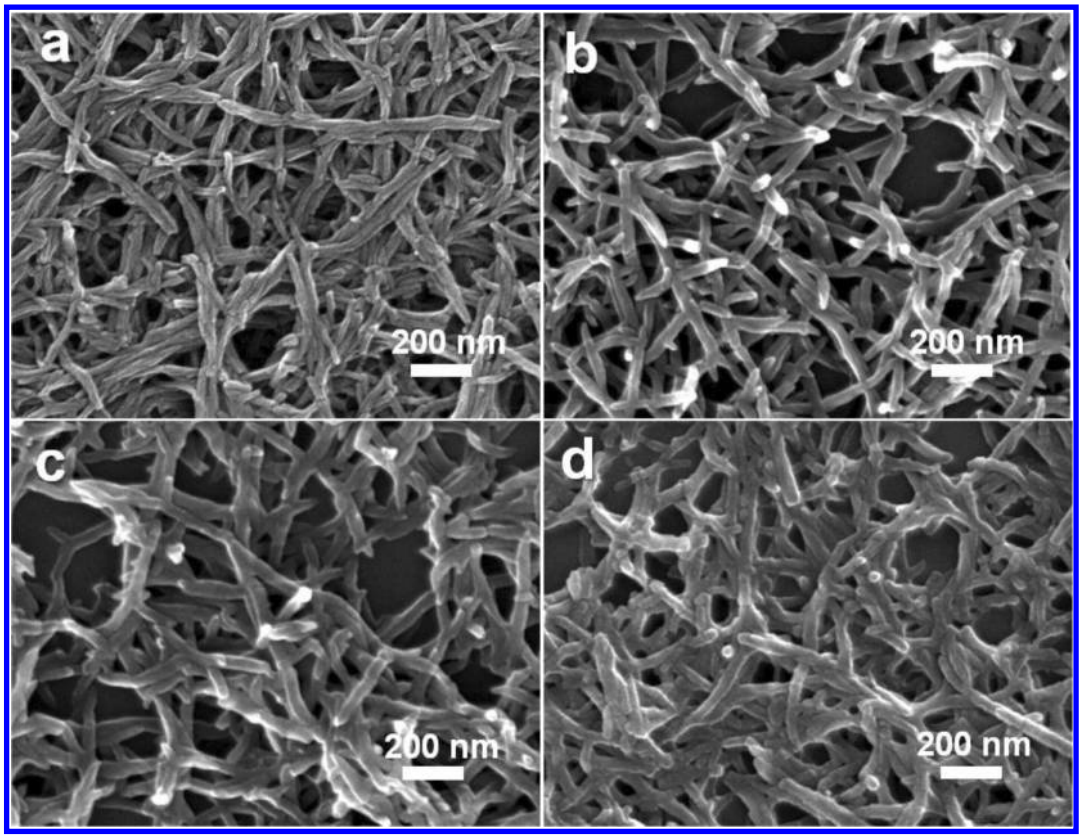

Figure 6. SEM images of SPANi synthesized with the following ASA/aniline molar ratios: (a) 0/100, (b) 30/100, (c) 50/50, and (d) 70/100 in the presence of 2.5 mol % *N*-phenyl-*p*-phenylenediamine per comonomer in 1.0 mol/L HCl.

UV−vis absorption maximum (λ_{max}), product yield, and conductivity of SPANi nanostructures, are presented in Table 1. As the ASA/aniline molar ratio is increased from 0/100 to 30/70 to 50/50 and to 70/30, the product yield of the polymers after dialysis decreased from 45.9 to 43.3 to 34.5 and to 20.4%, while the conductivity increased from 3.3×10^{-8} to 2.4×10^{-3} to 3.0×10^{-3} and to 5.7×10^{-3} S/cm, respectively. This is consistent with increasing ASA content, which results in a larger presence of sulfonic acid groups bonded to PANi, and leads to better water-solubility and higher self-doping-levels for the conjugated polymers. On the other hand, adding more ASA to copolymerize with aniline may generate copolymers with relatively low molecular weights, which would be easier to filter out during the dialysis. Both reasons may explain why the conductivities increase and the product yields of SPANi decrease.

The effect of the acidic media on the morphology, size, λ_{max}, product yield and conductivity of SPANi nanostructures is displayed in Table 2. Even when different acids are used such as hydrochloric acid (HCl), nitric acid (HNO_3), sulfuric acid (H_2SO_4), perchloric acid ($HClO_4$), camphorsulfonic acid (CSA) or *p*-toluenesulfonic acid (*p*-TSA), the obtained polymers exhibit a relatively stable product yield of 27−35%. Surprisingly, when aqueous HNO_3 is used as the polymerization medium, the self-doped SPANi also shows 6 orders of magnitude higher conductivity at neutral pH than conventional PANi with values up to 1.2×10^{-2} S/cm.

Several representative 2-substituted aniline derivatives were chosen to copolymerize with ASA in an HCl medium. The effect of the 2-substituents on the morphology, size, λ_{max}, product yield and conductivity of SPANi nanostructures is listed in Table 3. Since product yield and conductivity of SPANi largely depend on the aniline derivatives used for copolymerization, it is not surprising to find that different 2-substituents affect these characteristics. For example, when aniline derivatives like 2-chloroaniline, 2-methylaniline, 2-hydroxylaniline, 2-methoxyaniline, 2-methylthioaniline and 2-ethoxyaniline are used, the product yields of SPANi are 1.7, 24.2, 7.8, 32.9, 22.8 and 30.8%, while the conductivities achieved are 3.3×10^{-6}, 6.0×10^{-7}, 2.9×10^{-7}, 8.3×10^{-4}, 1.4×10^{-5} and 6.9×10^{-5} S/cm, respectively. Note that, the electron-donating capacities (ED) of the substituents -Cl, $-CH_3$, $-OH$, $-OCH_3$, $-SCH_3$ and $-OCH_2H_5$ follow the order: $ED_{Cl} < ED_{CH_3} < ED_{OH} < ED_{OCH_3} < ED_{SCH_3} < ED_{OC_2H_5}$, which suggests that the chain growth and elongation process readily occurs with 2-ethoxyaniline, 2-methylmercaptoaniline and 2-methoxyaniline in contrast to 2-chloroaniline, 2-methylaniline and 2-hydroxyaniline. It should also be noted that in terms of occupied volume (V), the substituents of $-Cl$, $-CH_3$, $-OH$, $-OCH_3$, $-SCH_3$ and $-OC_2H_5$ have the following order: $V_{OH} < V_{Cl} < V_{CH_3} < V_{OCH_3} < V_{SCH_3} < V_{OC_2H_5}$. The polymerization rate and $\pi-\pi$ stacking will be limited by steric hindrance as a result of increasing substituent size. This implies that the generated polymeric chains will be relatively more twisted and possess less planarity and π-conjugation in the case of 2-ethoxyaniline, thereby impairing the electron-transport properties. Both electron-donating and volume effects may be the reasons that SPANi exhibits the highest product yield and conductivity when 2-methoxyaniline is used for the reaction.

The dispersibility of SPANi nanostructures was qualitatively investigated by dispersing the products in various solvents.

dx.doi.org/10.1021/ma2024446 | *Macromolecules* 2012, 45, 1570−1579

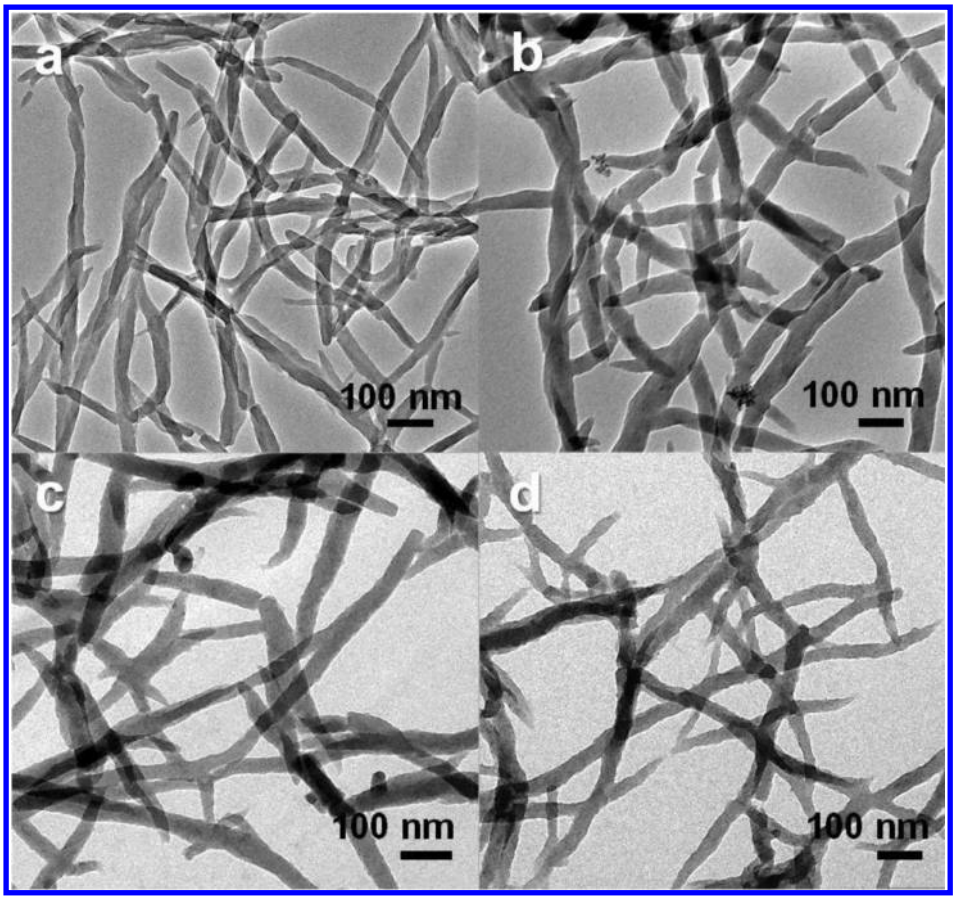

Figure 7. TEM images of SPANi synthesized with the following ASA/aniline molar ratios: (a) 0/100, (b) 30/70, (c) 50/50, and (d) 70/30 in the presence of 2.5 mol % *N*-phenyl-*p*-phenylenediamine per comonomer in 1.0 mol/L HCl.

Note that, SPANi nanostructures can be dispersed in many aqueous solvents such as DI water, alcohol, dilute acids and organic solvents such as *N*-methyl-2-pyrrolidone (NMP), *N,N*-dimethylformamide (DMF) and *N,N*-dimethylacetamide (DMAc). In particular, the nanocolloids produced can be completely stable in DI water for at least 4 weeks.

Chemical Composition. *UV–Vis Spectra.* The UV–vis spectra of aqueous dispersions of SPANi nanofibers in their acid doped salt form synthesized in HCl at variable ASA/aniline molar ratios are shown in Figure 1b–d. For comparison, the spectrum of pristine PANi nanofibers in their salt form is also presented (Figure 1a). The pristine PANi exhibits two characteristic peaks at 345 and 790 nm, while SPANi consisting of ASA and aniline exhibits two peaks at 295 and >845 nm, respectively, that can be attributed to the $\pi-\pi^*$ transition of the benzene rings and the $n-\pi^*$ transition of the quinoid rings,[5] respectively. For the emeraldine base form of oligoaniline systems, some recent theoretical work suggests that the peak at relative higher wavelength can also be attributed to the $\pi-\pi^*$ transition of the quinoid rings, according to extensive density functional theory (DFT) calculations.[27] With an increase in the ASA/aniline molar ratio from 0/100 to 30/70 to 50/50 and to 70/30, the peak due to the $n-\pi^*$ transition red shifts from 790 to 845 to 856 and to 870 nm, indicating that the ASA has been copolymerized with aniline. The exciton band near 800 nm undergoes a large red shift when more ASA is used in the copolymerization, signifying an increase in the $\pi-\pi^*$ conjugation and a decrease in the bandgap.

The UV–vis spectra of SPANi nanofibers in their salt form synthesized at an ASA/aniline molar ratio of 50/50 in the presence of different acidic media are shown in Figure 2. When using acidic media such as HNO_3, H_2SO_4, $HClO_4$, CSA, and *p*-TSA, SPANi displays $n-\pi^*$ transition peaks at 858, 853, 920, 853, and 873 nm, respectively, compared to 853 nm for the product obtained with HCl. This means that the conjugation length of SPANi depends on the acidic medium utilized. The reason may be that different acids change the solubility of the monomers and initiators, which also affect the copolymerization activity of the ASA and aniline leading to variable molecular weights of SPANi.

A series of SPANi nanostructures with various 2-substituents such as $-Cl$, $-CH_3$, $-SCH_3$, $-OCH_3$, $-OC_2H_5$, and $-OH$ were obtained by copolymerizing the ASA monomer with aniline derivatives at the same molar ratio of 50/50 in HCl. With increasing electron-donating ability of the substituents from $-Cl$ to $-CH_3$ to $-SCH_3$ to $-OCH_3$ and to $-OC_2H_5$, the λ_{max} values of the corresponding SPANi red shift from 765 to 825 to 858 to 870 and to 873 nm, respectively, as shown in Figure 3. Essentially the stronger the electron-donating substituent that is introduced, the larger the charge density that is created on the SPANi polymer backbone; as a result, the copolymer will adapt a more linear morphology, and thus increase the $\pi-\pi$ conjugation. Note that the UV–vis spectrum of the product synthesized from ASA and 2-hydroxylaniline shows a peak at a maximum wavelength of 418 nm. Generally, the more 2-hydroxylaniline monomers that are copolymerized with ASA, the greater the water-solubility of SPANi with a

dx.doi.org/10.1021/ma2024446 | *Macromolecules* 2012, 45, 1570–1579

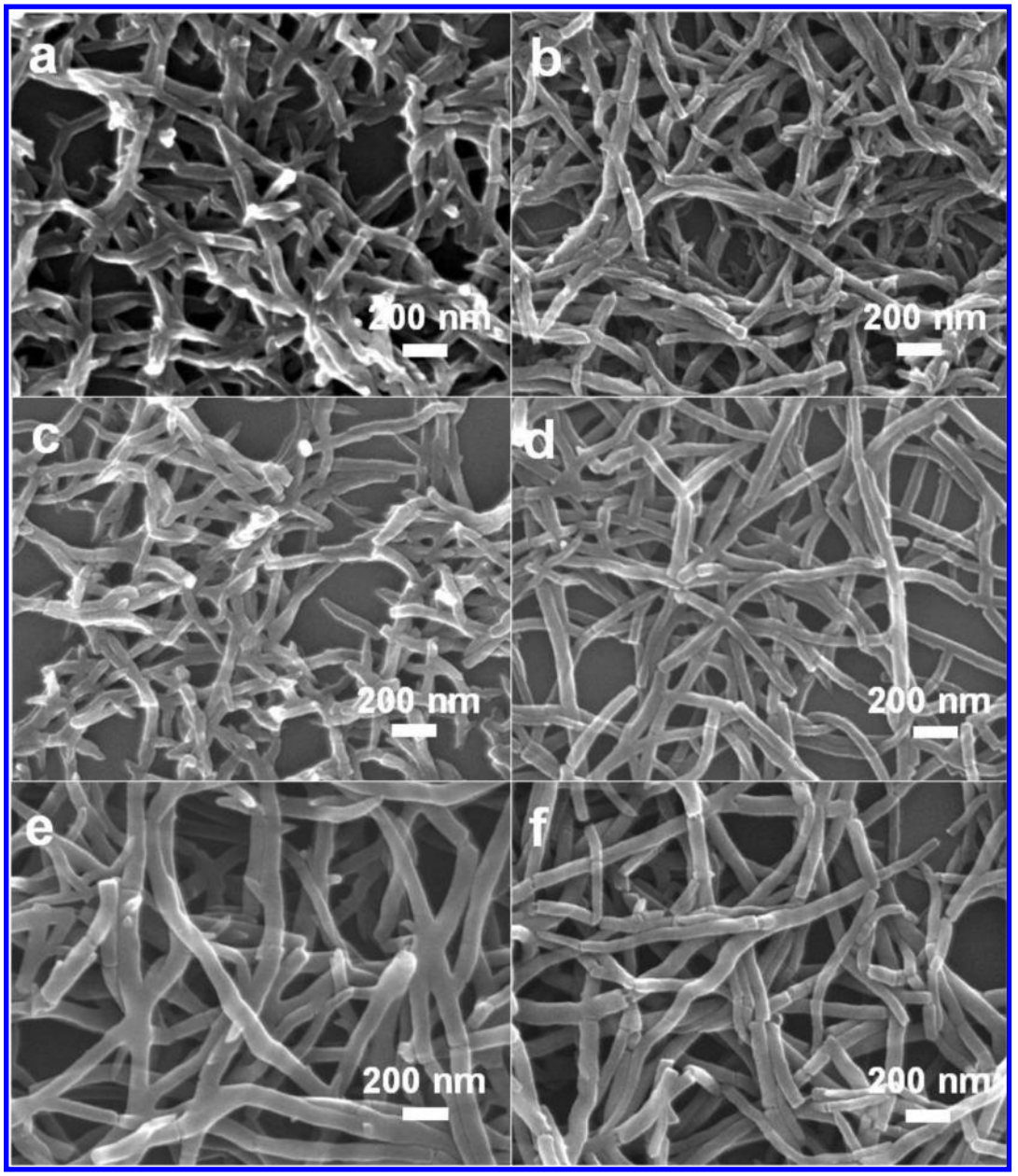

Figure 8. SEM images of SPANi synthesized in the following acidic medium: (a) HCl, (b) H_2SO_4, (c) CSA, (d) HNO_3, (e) $HClO_4$, or (f) *p*-TSA in the presence of 2.5 mol % *N*-phenyl-*p*-phenylenediamine per comonomer in 1.0 mol/L HCl, at a fixed ASA/aniline molar ratio of 50/50.

higher molecular weight. The dialysis purification used here may leave behind some sulfonated oligoaniline with a few sulfonic acid groups. This also explains why when using 2-hydroxylaniline, a higher charge density molecule than both 2-chloroaniline and 2-methylaniline, the resulting product displays far lower $\pi-\pi$ conjugation than other lower charge density molecules.

ATR-FT-IR Spectra. Figure 4b–g displays ATR-FT-IR spectra of SPANi nanostructures synthesized by copolymerizing the ASA monomer and aniline derivatives such as 2-chloroaniline, 2-methylaniline, 2-hydroxylaniline, 2-methoxyaniline, 2-methylmercaptoaniline and 2-ethoxyaniline at a comonomer ratio of 50/50 in HCl. For comparison, the spectrum of pristine PANi nanofibers in their emeraldine base form is also presented (Figure 4a). The pristine emeraldine base PANi nanofibers give characteristic IR peaks at 1587, 1493, 1289, and 1164 cm^{-1} corresponding to quinoid, benzenoid, C–N aromatic amine, and —N═quinoid═N— (electron-like band) stretching modes, respectively, which are in good agreement with a previous report.[26] The SPANi nanostructures, after dialysis in pH 5.5–6.0 for two months, show four typical IR peaks at 1205, 1084, 693, and 615 cm^{-1}, which can be assigned to the asymmetric and symmetric O–S–O stretching modes, and S–O and C–S stretching modes, respectively; these peaks do not differ significantly from that of conventional SPANi.[28,29] These characteristic bands are absent from the spectrum of pristine emeraldine base PANi, revealing that the sulfonic acid groups have been bonded to the aromatic rings in the SPANi polymeric chains.

XRD. X-ray diffraction patterns are presented in Figure 5 for SPANi nanostructures synthesized by copolymerizing ASA and aniline monomers at a molar ratio of 50/50 in acidic media of HCl, HNO_3, H_2SO_4, $HClO_4$, CSA, and *p*-TSA. The six types of SPANi powders are all nearly amorphous with

dx.doi.org/10.1021/ma2024446 | *Macromolecules* 2012, 45, 1570–1579

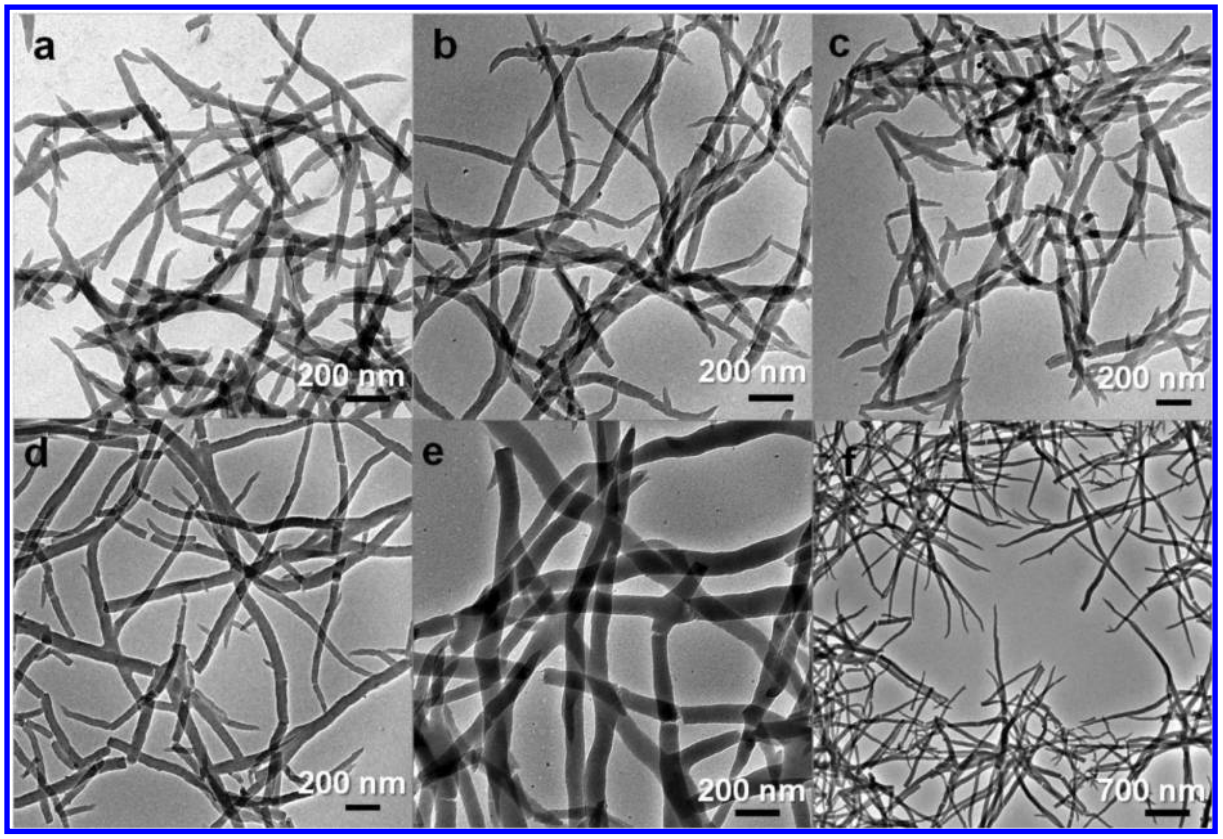

Figure 9. TEM images of SPANi synthesized in the following acidic medium: (a) HCl, (b) H_2SO_4, (c) CSA, (d) HNO_3, (e) $HClO_4$, or (f) *p*-TSA in the presence of 2.5 mol % *N*-phenyl-*p*-phenylenediamine per comonomer in 1.0 mol/L HCl, at a fixed ASA/aniline molar ratio of 50/50.

only a broad peak at 2θ = 21.5−23.1° that can be attributed to periodicity parallel and perpendicular to the semicrystalline PANi-like main chains.[30] Note that a minor peak around 2θ = 28° is observed for SPANi synthesized by $HClO_4$ (Figure 5d). This may correspond to classical $\pi-\pi$ stacking between aromatic rings of the more crystalline SPANi nanostructures. This result is consistent with rectangular nanoplates of oligoaniline induced by $HClO_4$.[31] By changing the size of the acidic dopants, the center of the peak exhibits a visible difference due to the variable supramolecular structures. Conducting polymer molecular chains are usually long and semirigid in sections. The dopant anions reside near the positively charged polymers due to ionic attractions. Thus, the dopants appear to affect the diameter of the nanofibers, and thus change their interchain packing distance and ultimately, the supramolecular structures.

Morphology, Size, and Dimensionality. Morphology, size and dimensionality control of organic nanostructures remains a significant challenge within the field of organic conductors and continues to draw much interest. SPANi synthesized by previously reported methods possesses a granular, agglomerated morphology.[28] By altering the ASA/aniline molar ratios, the aniline derivatives and the acid media, the morphology, nanosize and dimensionality of SPANi can be tuned by chemical oxidative polymerization of the monomers in the presence of the initiator, *N*-phenyl-*p*-phenylenediamine. SEM and TEM images of the resulting SPANi dispersions show that entangled nanofibers are created during this process (Figures 6 and 7). By increasing the ASA and aniline molar ratio from 0/100 to 70/30, the diameters, lengths and aspect ratios of the SPANi nanofibers change from 50 to 60 nm, 1.0 to 0.7 μm and 20.0 to 11.7 (Table 1), respectively. Increasing the number of ASA units in the SPANi chain produces shorter yet larger diameter nanofibers, which is likely due to the improved water-solubility. Note that the percentage of aniline can be as low as 10% to generate sulfonated polyaniline copolymer nanofibers. In addition, by adjusting the order in which the monomers are added, i.e. adding aniline first to form the nanofiber seeds and then ASA, we believe that the aniline and initiator will polymerize first, then the oxidant induces ASA to polymerize, finally producing PANi nanofibers doped by poly(o-aminobenzenesulfonic acid).

Previous studies have demonstrated that altering the size of the acid used is an effective method for tuning the size of polyaniline nanofibers and polypyrrole nanospheres,[32,33] and therefore, similar results were expected for SPANi nanofibers. The effect of the acidic medium on the size and nanomorphology of SPANi synthesized by an ASA/aniline molar ratio of 50/50 were examined by both SEM and TEM. When HCl, H_2SO_4 or CSA was used, entangled 1-D nanofibers formed and exhibit average diameters of 55−65 nm, lengths of 0.75−2.1 μm and aspect ratios of 13−34 (Figure 8a−c and Figure 9a−c). As the acidic medium is changed to HNO_3, $HClO_4$ or *p*-TSA, the resulting nanofibers possess average diameters and lengths with values up to 75 nm and 4.5 μm, Figure 8d−f and Figure 9d−f, respectively. These nanofibers are also less entangled and longer than nanofibers produced by HCl, H_2SO_4 or CSA. In particular, the aspect ratio of the partially arranged nanofibers is calculated to be as high as 60.0 when *p*-TSA was used (Table 2). As is well-known, when a conjugated polymer is doped with an acid, the polymeric chains become protonated and positively charged. The

dx.doi.org/10.1021/ma2024446 | *Macromolecules* 2012, 45, 1570−1579

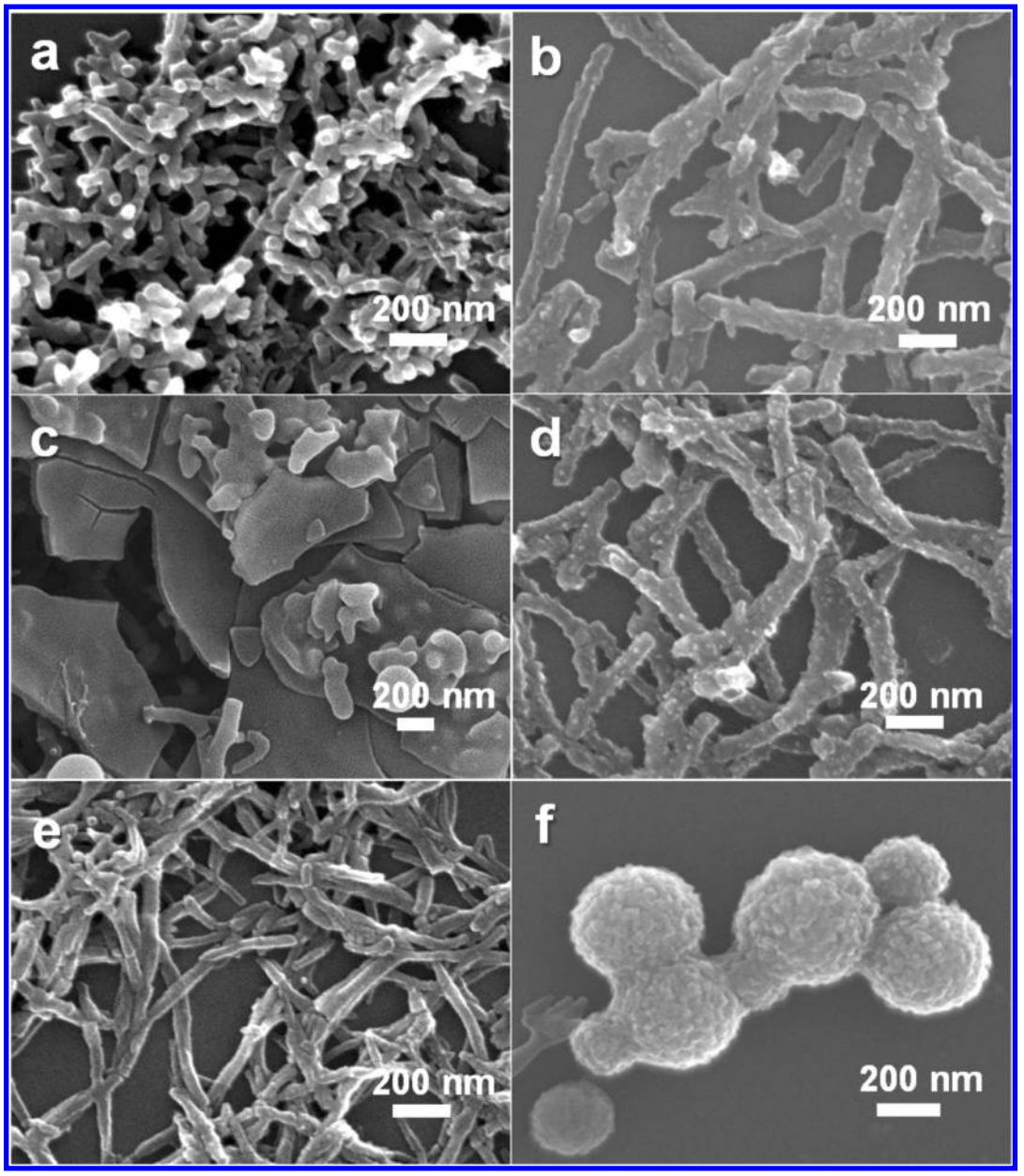

Figure 10. SEM images of SPANi synthesized with the following 2-substituted group (R) on aniline: (a) Cl, (b) OCH_3, (c) SCH_3, (d) OC_2H_5, (e) CH_3, or (f) OH in the presence of 2.5 mol % *N*-phenyl-*p*-phenylenediamine per comonomer in 1.0 mol/L HCl, at a fixed ASA/aniline ratio of 50/50.

negatively charged dopant anions reside near the positively charged polymer backbone due to ionic attractions. The size and charge density of the doping acids thus influence the interchain packing distance and ultimately the supramolecular morphology. Moreover, different acids also change the solubility of the initiator, monomers and as-formed polymers/oligomers, which also affect the diameters of the resulting nanofibers. This explains why the dopant-induced nanoscale morphology controls the size of SPANi.

In addition, the nanomorphology and dimensionality of SPANi can be readily tuned by choosing aniline derivatives with different 2-substituents. When ASA was copolymerized with aniline derivatives like 2-chloroaniliene, 2-methylaniline, 2-methoxyaniline, 2-ethoxyaniline, 2-methylmercaptoaniline, or 2-hydroxyaniline at the same molar ratio of 50/50, the SPANi formed displays drastically different morphologies of 1-D nanofibers, 1-D nanosticks, 1-D nanothorns, 1-D nanorods, 2-D nanoplates, or 3-D nanospheres (Figure 10), respectively. TEM images of SPANi confirm that the nanomorphology and dimensionality are similar to their SEM images (Figure 11). Interestingly, the TEM images show that porous nanospheres have been created by copolymerizing ASA and 2-hydroxylaniline. The substituent groups dramatically control the basic morphology of SPANi synthesized using the rapid initiated copolymerization. This phenomenon is consistent with the results reported for pristine PANi synthesized using both interfacial polymerization and rapidly mixed reactions.[34] The differences in morphology observed among these aniline derivatives when copolymerizing these monomers with ASA suggests that the basicity, solubility, redox potential and bulk volume of the monomers affect which nanostructures are observed: 1-D nanofibers, 1-D nanosticks,

dx.doi.org/10.1021/ma2024446 | *Macromolecules* 2012, 45, 1570−1579

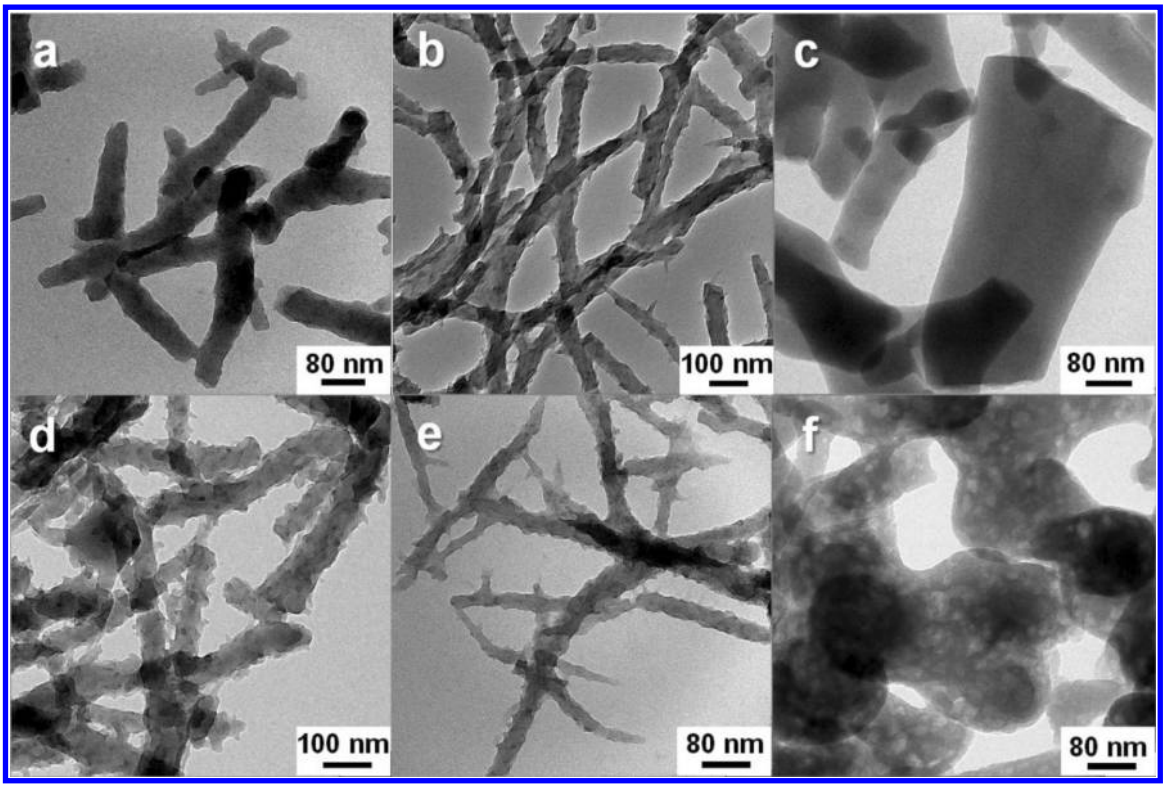

Figure 11. TEM images of SPANi synthesized with the following 2-substituted group (R) on aniline: (a) Cl, (b) OCH_3, (c) SCH_3, (d) OC_2H_5, (e) CH_3, or (f) OH in the presence of 2.5 mol % *N*-phenyl-*p*-phenylenediamine per comonomer in 1.0 mol/L HCl, at a fixed ASA/aniline derivative ratio of 50/50.

1-D nanothorns, 1-D nanorods, 2-D nanoplates, or 3-D nanospheres.

■ CONCLUSIONS

We have successfully synthesized a variety of sulfonated polyaniline (SPANi) nanostructures via rapid initiated copolymerization of *o*-aminobenzenesulfonic acid and aniline or aniline derivatives in the presence of a catalytic amount of *N*-phenyl-*p*-phenylenediamine in an acidic medium. The nanomorphology, dimensionality, chemical composition and electrical properties of SPANi were systemically characterized using SEM, TEM, UV−vis, ATR-FT-IR, XRD, and two-point probe techniques. By regulating the comonomer molar ratios, aniline derivatives used and acid media employed, 1-D nanofibers, nanosticks, nanothorns, and nanorods, 2-D nanoplates and 3-D porous nanospheres of SPANi are readily generated. In particular, the SPANi nanofibers exhibit length and aspect ratios with values up to 4.5 μm and 60, respectively, making the fabrication of single-wire devices and postsynthetic alignment possible. The SPANi nanostructures can be easily processed in many aqueous or organic solvents such as DMF, and demonstrate much better conductivity at pH values of 5.5−6.0 than their polyaniline counterparts (10^{-2} S/cm vs 10^{-8} S/cm). The SPANi nanostructures are therefore ideal candidates for electrode materials for the development of high-performance, high-power and flexible bioelectronic devices.

■ AUTHOR INFORMATION

Corresponding Author

*E-mail: (R.B.K.) kaner@chem.ucla.edu; (X.W.) wangxia@usst.edu.cn.

Notes

The authors declare no competing financial interest.

■ ACKNOWLEDGMENTS

Financial support from Abraxis Bioscience now CalCap Equity (RBK), the China Scholarship Council No. 2008626064, the Starting Fund from the University of Shanghai for Science and Technology (10-00-310-001), the Key Project of Science and Technology of Shanghai Commission (No. 10JC1411700) and the National Natural Science Foundation of China (No. 50873077) (Y.Z.L.) are gratefully acknowledged.

■ REFERENCES

(1) Li, D.; Huang, J. X.; Kaner, R. B. Polyaniline nanofibers: A unique polymer nanostructure for versatile applications. *Acc. Chem. Res.* **2009**, *42* (1), 135−145.

(2) Tran, H. D.; Li, D.; Kaner, R. B. One-dimensional conducting polymer nanostructures: Bulk synthesis and applications. *Adv. Mater.* **2009**, *21* (14−15), 1487−1499.

(3) Tran, H. D.; D'Arcy, J. M.; Wang, Y.; Beltramo, P. J.; Strong, V.; Kaner, R. B. The oxidation of aniline to produce "polyaniline": A process yielding many different nanoscale structures. *J. Mater. Chem.* **2011**, *21* (11), 3534−3550.

(4) Thiyagarajan, M.; Samuelson, L. A.; Kumar, J.; Cholli, A. L. Helical conformational specificity of enzymatically synthesized water-soluble conducting polyaniline nanocomposites. *J. Am. Chem. Soc.* **2003**, *125* (38), 11502−11503.

(5) Huang, J. X.; Virji, S.; Weiller, B. H.; Kaner, R. B. Polyaniline nanofibers: Facile synthesis and chemical sensors. *J. Am. Chem. Soc.* **2003**, *125* (2), 314−315.

(6) MacDiarmid, A. G. Synthetic metals": A novel role for organic polymers (Nobel Lecture). *Angew. Chem., Int. Ed.* **2001**, *40* (14), 2581−2590.

(7) Yue, J.; Epstein, A. J. Synthesis of self-doped conducting polyaniline. *J. Am. Chem. Soc.* **1990**, *112* (7), 2800−2801.
(8) Lee, W.; Du, G.; Long, S. M.; Epstein, A. J.; Shimizu, S.; Saitoh, T.; Uzawa, M. Charge transport properties of fully-sulfonated polyaniline. *Synth. Met.* **1997**, *84* (1−30), 807−808.
(9) Ito, S.; Murata, K.; Teshima, S.; Aizawa, R.; Asako, Y.; Takahashi, K.; Hoffman, B. M. Simple synthesis of water-soluble conducting polyaniline. *Synth. Met.* **1998**, *96* (2), 161−163.
(10) Hwang, G. W.; Chen, S. A. Structure characterization of self-acid-doped sulfonic acid ring-substituted polyaniline in its aqueous solutions and as solid film. *Macromolecules* **1996**, *29* (11), 3950−3955.
(11) Yamamoto, T.; Ushiro, A.; Yamaguchi, I.; Sasaki, S. Synthesis, structure, and chemical properties of lithium salts of poly-(2-methoxyaniline-5-sulfonic acid). *Macromolecules* **2003**, *36* (19), 7075−7081.
(12) Pornputtkul, Y.; Strounina, E. V.; Kane-Maguire, L. A. P.; Wallace, G. G. Redox behavior of poly(2-methoxyaniline-5-sulfonic acid) and its remarkable thermochromism, solvatochromism, and ionochromism. *Macromolecules* **2010**, *43* (23), 9982−9989.
(13) Rahmanifar, M. S.; Mousavi, M. F.; Shamsipur, M. Effect of self-doped polyaniline on performance of secondary Zn−polyaniline battery. *J. Power Sources* **2002**, *110* (1), 229−232.
(14) Yang, C. H.; Chih, Y. K. Molecular assembled self-doped polyaniline interlayer for application in polymer light-emitting diode. *J. Phys. Chem. B* **2006**, *110* (39), 19412−19417.
(15) Huh, P.; Kim, S. C.; Kim, Y. H.; Wang, Y. P.; Singh, J.; Kumar, J.; Samuelson, L. A.; Kim, B. S.; Jo, N. J.; Lee, J. O. Optical and electrochemical detection of saccharides with poly(aniline-co-3-aminobenzeneboronic acid) prepared from enzymatic polymerization. *Biomacromolecules* **2007**, *8* (11), 3602−3607.
(16) Ali, S. R.; Ma, Y. F.; Parajuli, R. R.; Balogun, Y.; Lai, W. Y. C.; He, H. X. A nonoxidative sensor based on a self-doped polyaniline/carbon nanotube composite for sensitive and selective detection of the neurotransmitter dopamine. *Anal. Chem.* **2007**, *79* (6), 2583−2587.
(17) Yang, Y. Y.; Min, Y.; Wu, J-C.; Hansford, D. J.; Feinberg, S. E.; Epstein, A. J. Synthesis and Characterization of Cytocompatible Sulfonated Polyanilines. *Macromol. Rapid Commun.* **2011**, *32* (12), 887−892.
(18) Silva, W. J. D.; Hümmelgen, I. A. Mello RMO. Sulfonated polyaniline/n-type silicon junctions. *J. Mater. Sci.* **2009**, *20* (2), 123−126.
(19) Yang, C. H.; Chih, Y. K.; Wu, W. C.; Chen, C. H. Molecular assembly engineering of self-doped polyaniline film for application in electrochromic devices. *Electrochem. Solid-State Lett.* **2006**, *9* (1), C5−C8.
(20) Masdarolomoor, F.; Innis, P. C.; Ashraf, S.; Kaner, R. B.; Wallace, G. G. Nanocomposites of polyaniline/poly(2-methoxyaniline-5-sulfonic acid). *Macromol. Rapid Commun.* **2006**, *27* (23), 1995−2000.
(21) Li, X. G.; Lü, Q. F.; Huang, M. R. Self-stabilized nanoparticles of intrinsically conducting copolymers from 5-sulfonic-2-anisidine. *Small* **2008**, *4* (8), 1201−1209.
(22) Deore, B. A.; Yu, I.; Freund, M. S. A switchable self-doped polyaniline: Interconversion between self-doped and non-self-doped forms. *J. Am. Chem. Soc.* **2004**, *126* (1), 52−53.
(23) Yu, I.; Deore, B. A.; Recksiedler, C. L.; Corkery, T. C.; Abd-El-Aziz, A. S.; Freund, M. S. Thermal stability of high molecular weight self-doped poly(anilineboronic acid). *Macromolecules* **2005**, *38* (24), 10022−10026.
(24) Gupta, B.; Prakash, R. Synthesis of functionalized conducting polymer "polyanthranilic acid" using various oxidizing agents and formation of composites with PVC. *Polym. Adv. Technol.* **2011**, *22* (12), 1982−1988.
(25) Chan, H. S. O.; Ho, P. K. H.; Ng, S. C.; Tan, B. T. G.; Tan, K. L. A new water-soluble, self-doping conducting polyaniline from poly(o-aminobenzylphosphonic acid) and its sodium salts: Synthesis and characterization. *J. Am. Chem. Soc.* **1995**, *117* (33), 8517−8523.
(26) Liao, Y. Z.; Zhang, C.; Zhang, Y.; Strong, S.; Tang, J. S.; Li, X. G.; Kalantar-zadeh, K.; Hoek, E. M. V.; Wang, K. L.; Kaner, R. B. Carbon nanotube/polyaniline composite nanofibers: Facile synthesis and chemosensors. *Nano Lett.* **2011**, *11* (3), 954−959.
(27) Shao, Z. F.; Rannou, P.; Sadki, S.; Fey, F.; Lindsay, D. M. Faul CFJ. Delineating poly(Aniline) redox chemistry by using tailored oligo(aryleneamine)s: Towards oligo(aniline)-based organic semiconductors with tunable optoelectronic properties. *Chem.—Eur. J.* **2011**, *17* (44), 12512−12521.
(28) Mu, S. L. Polyaniline with two types of functional groups: Preparation and characteristics. *Macromol. Chem. Phys.* **2005**, *206* (6), 689−695.
(29) Li, G. C.; Zhang, C. Q.; Peng, H. R.; Chen, K. Z.; Zhang, Z. K. Hollow self-doped polyaniline micro/nanostructures: Microspheres, aligned pearls, and nanotubes. *Macromol. Rapid Commun.* **2008**, *29* (24), 1954−1958.
(30) Wang, Y.; Tran, H. D.; Liao, L.; Duan, X.; Kaner, R. B. Nanoscale Morphology, Dimensional Control, and Electrical Properties of Oligoanilines. *J. Am. Chem. Soc.* **2010**, *132* (30), 10365−10373.
(31) Xia, H. S.; Wang, Q. Ultrasonic irradiation: A novel approach to prepare conductive polyaniline/nanocrystalline titanium oxide composites. *Chem. Mater.* **2002**, *14* (5), 2158−2165.
(32) Huang, J. X.; Kaner, R. B. A general chemical route to polyaniline nanofibers. *J. Am. Chem. Soc.* **2004**, *126* (3), 851−855.
(33) Liao, Y. Z.; Li, X. G.; Kaner, R. B. Facile synthesis of water-dispersible conducting polymer nanospheres. *ACS Nano* **2010**, *4* (9), 5193−5202.
(34) Huang, J. X.; Kaner, R. B. The intrinsic nanofibrillar morphology of polyaniline. *Chem. Commun.* **2006**, *4*, 367−376.